Mineralogy of the Rock Canyon Creek REE-fluorite deposit, British Columbia, Canada

Mihoko Hoshino[1, a], Yoshiaki Kon[1], Shinsuke Kodama[1], George J. Simandl[2, 3], Suzanne Paradis[4], Craig Green[2], Chizu Namatame[1], Izumi Matsunaga[1], and Tetsuichi Takagi[1]

[1] Mineral Resource Research Group, National Institute of Advanced Industrial Science and Technology, Tsukuba, Japan
[2] School of Earth and Ocean Sciences, University of Victoria, BC, V8P 5C2
[3] British Columbia Geological Survey, Ministry of Energy and Mines, Victoria, BC, V8W 9N3
[4] Geological Survey of Canada, Natural Resources Canada, Sidney, BC, V8L 4B2
[a] corresponding author: hoshino-m@aist.go.jp

Recommended citation: Hoshino, M., Kon, Y., Kodama, S., Simandl, G.J., Paradis, S., Green, C., Namatame, C., Matsunaga, I., and Takagi, T., 2017. Mineralogy of the Rock Canyon Creek REE-Fluorite Deposit, British Columbia, Canada. In: Geological Fieldwork 2016, British Columbia Ministry of Energy and Mines, British Columbia Geological Survey Paper 2017-1, pp. 205-213.

Abstract

The main REE-fluorite mineralized zone at the Rock Canyon Creek deposit was intersected by drilling along a strike length of 1100 metres and to a depth of more than 124 metres. Samples of drill core from this zone were analyzed by SEM-EDS, powder-XRD and Raman Spectroscopy. Mineralization consists of dolomite, fluorite, quartz, K-feldspar, barite, porous apatite, pyrite, REE-bearing fluorocarbonates [bastnäsite-(Ce), parisite-(Ce), synchysite-(Ce)], and REE-bearing phosphates [monazite-(Ce), crandallite group minerals] in various proportions. Barite and fluorite veinlets and those containing REE minerals, fluorite, barite and pyrite are cut by calcite-filled fractures. REE carbonates and REE phosphates are spatially associated with pyrite, barite and fluorite. Most of the pyrite in weathered surface samples is replaced by hematite. Preliminary results indicate that the bastnäsite-(Ce) contains 8.7 to 26.7 wt.% La, 24.3 to 34.4 wt.% Ce, from detection limit to 4.7 wt.% Pr, 8.2 to 24.1 wt.% Nd, undetected to 2.84 wt.% Sm, and undetected to 8.42 wt.% Th. Synchysite-(Ce) contains 5.2 to 17.4 wt.% La, 16.6 to 25.3 wt.% Ce, undetected to 8.3 wt.% Pr, 2.6 to 19.4 wt.% Nd, undetected to 2.13 wt.% Y, and undetected to 3.7 wt.% Th. Monazite contains 11.03 to 13.03 wt.% P, 14.15 to 18.95 wt.% La, 21.46 to 32.98 wt.% Ce, 4.01 to 8.80 wt.% Nd, and undetected to 3.55 wt.% Th. The monazite-(Ce) grains analyzed include impurity elements like Al, and Ca, suggesting that monazite-(Ce) is altered or formed in the supergene environment. Cross cutting relationships and replacement textures suggest that REE-bearing carbonates, fluorite, barite and pyrite are of hydrothermal origin.

Keywords: Rare earth elements, hydrothermal, bastnäsite, synchysite, parisite, crandallite group minerals, monazite, fluorite, barite

1. Introduction

The Rock Canyon Creek rare earth element (REE)-fluorite deposit, about 90 km north-northeast of Cranbrook is in the British Columbia alkaline province (Fig. 1). Most of the 44 REE occurrences reported in British Columbia (Simandl et al., 2012) are in this province which consists of carbonatites, nepheline and sodalite syenites, ijolite series rocks, kimberlite, and many ultramafic and lamprophyre diatremes, breccias, and dikes (Pell, 1994). The Rock Canyon Creek deposit is hosted by Middle Devonian carbonate rocks of the Cedared and Burnais formations (Pell and Hora, 1986; Green et al., 2017). The main REE-fluorite mineralized zone (Fig. 2) was investigated at depth by 17 diamond-drill holes totalling 1213.79 metres (Pighin et al., 2010). The steeply dipping REE-fluorite zone extends along strike for more than 1100 metres, to a depth greater than 124 metres; it remains open along strike and dip and, at least locally, is more than 50 metres thick. In this study, we carried out a detailed mineral identification of selected mineralized samples from the drill hole RCC-09-14 and report the results.

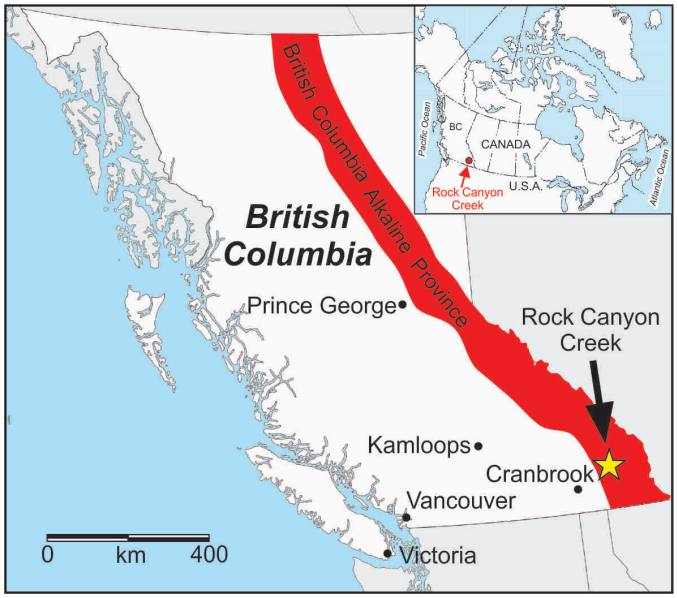

Fig. 1. Location of the Rock Canyon Creek REE-fluorite deposit. The British Columbia Alkaline Province, as defined by Pell (1994), is shown in red.

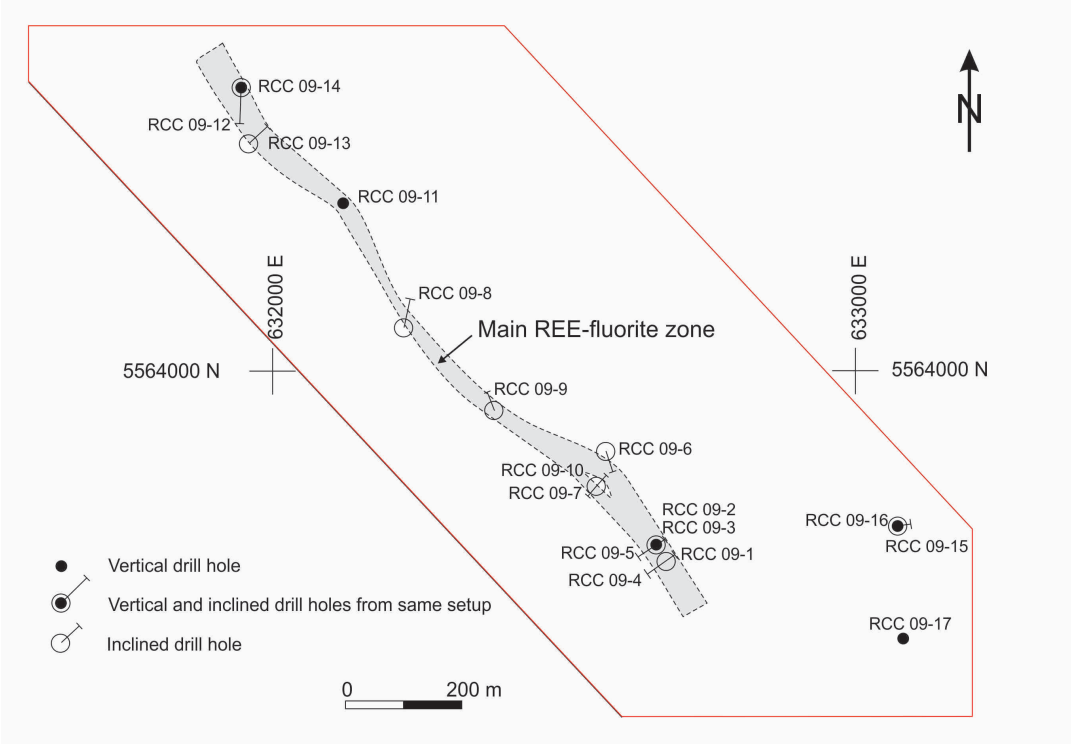

Fig. 2. Approximate vertical projection of the main REE-fluorite mineralized zone to the surface and locations of diamond-drill holes. Compiled from Pighin (2010). Mineralized zone is open at depth and along strike in both directions. Drill hole RCC-09-14, the main object of this study, intersected high-grade mineralization and is one of the two northernmost drill holes.

2. Analytical methods

Fifteen polished thin sections were prepared from core of the drill hole RCC-09-14. Selected minerals were analyzed using energy dispersive spectroscopy on a scanning electron microscope (SEM-EDS; JEOL JSM-6610LV) and Raman spectroscopy analysis (JASCO NRS-5100) was carried out for mineral identification on selected thin sections. Core samples, representing 3-metre drill core intervals, from drill hole RCC-09-14 were crushed, split, and milled to make powder samples for powder X-ray diffraction (Powder-XRD). Qualitative powder-XRD analyses were conducted on 38 powdered samples using the Rigaku Smart Lab X-ray diffractometer. The operating voltage and current were 40 kV and 200 mA, respectively, and samples were scanned from 3º to 70º 2θ at a step size of 0.02º and scan speed of 10º min^{-1}. Mineral identification using the XRD data was conducted by using PDXL database fitting program (ver. 2.7.2). All analytical work was carried out at the Mineral Resource Research Group of National Institute of Advanced Industrial Science and Technology in Tsukuba, Japan.

3. Results

3.1. X-ray diffraction analysis

The main minerals identified by X-ray diffraction analysis (Powder-XRD) are dolomite, fluorite, barite and pyrite (Table 1). Quartz was in 30 of 38 samples. Bastnäsite was detected by Powder-XRD and SEM-EDS, and was identified as the main REE mineral in 50% of the analyzed samples at depths of 1 to 6 m, 15 to 45 m and 114 to 124.7 m. The occurrence of bastnäsite is consistent with SEM-EDS results (Tables 1, 2). Monazite was only detected in two of the 3 metre-long samples. Apatite was detected from the 114-117 m and 123-124.7 m intervals.

3.2. SEM-EDS analysis

Following the qualitative analysis, quantitative analysis of minerals was conducted using SEM-EDS (JEOL JSM-6610LV). SEM-EDS analyses were carried out on 15 thin sections (Table 2). Cobalt (Co) standard was used for quantitative analysis. These analyses identified dolomite, fluorite, quartz, K-feldspar, barite, apatite, pyrite, REE-bearing fluorocarbonates [(bastnäsite-(Ce), parisite-(Ce) and synchysite-(Ce)], and REE phosphates [monazite-(Ce) and crandallite group minerals]. REE-bearing fluorocarbonates were identified in 14 samples, and REE phosphates in 9. Both REE carbonates and REE phosphates are commonly spatially associated with pyrite, barite and fluorite (Figs. 3a-f). Representative chemical compositions are summarized in Table 3 for bastnäsite-(Ce), Table 4 for synchysite-(Ce), Table 5 for parisite-(Ce), Table 6 for monazite-(Ce), and Table 7 for crandallite group minerals.

Pyrite is one of most common minerals in samples from drill hole RCC-09-14. It commonly occurs as aggregates of small euhedral pyrite grains (Figs. 3 a, d, e) with rims replaced by hematite (Fig. 3a). Barite and fluorite form crystals in

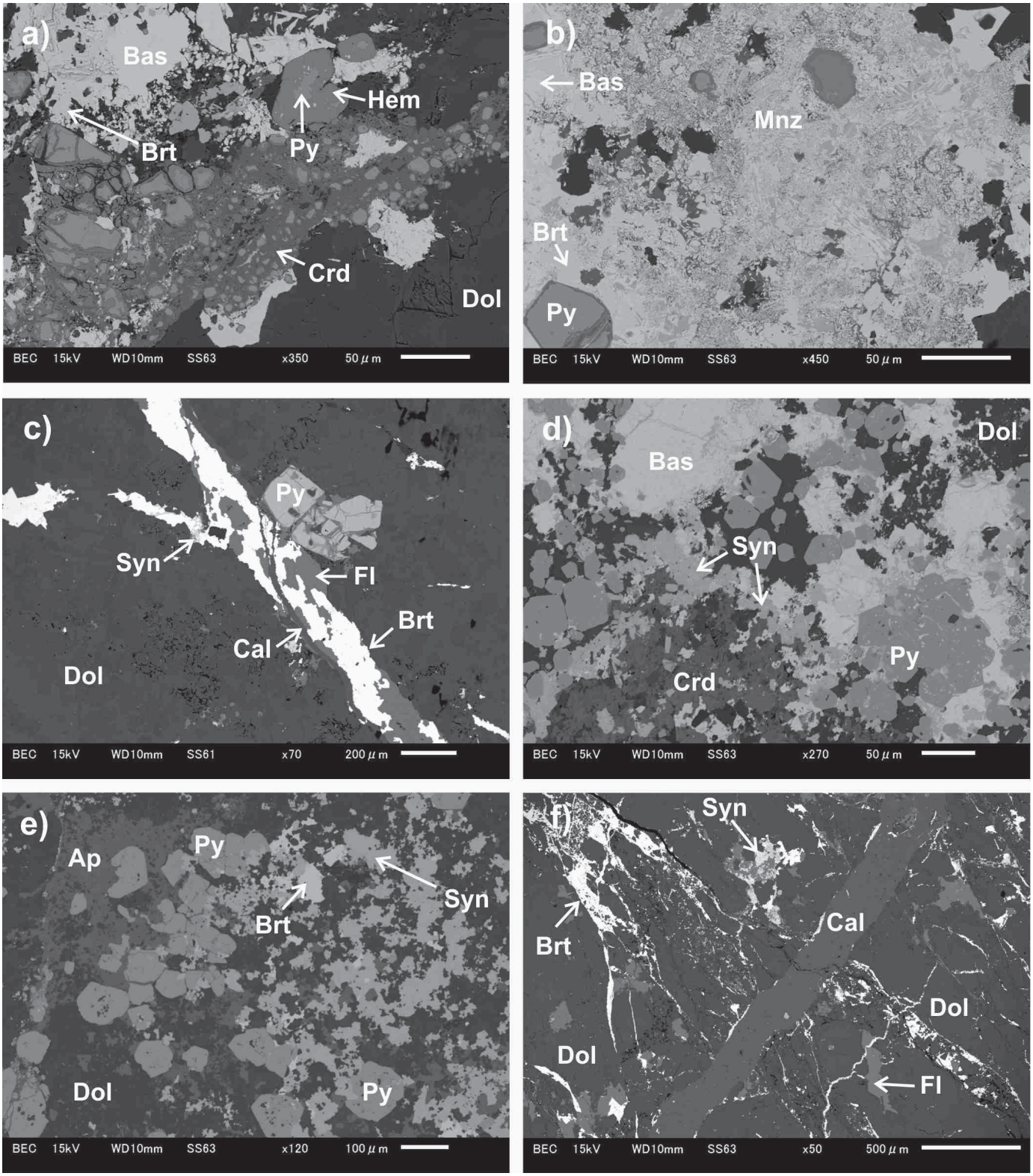

Fig. 3. Back-scatter-electron images of representative textures in drill hole RCC-09-14. **a)** RCC-09-14-1 m, bastnäsite-(Ce) with pyrite, hematite, barite, and crandallite. **b)** RCC-09-14-1 m, mixture of monazite-(Ce), bastnäsite-(Ce) and barite. **c)** RCC-09-14-1 m, late calcite-filled hairline fractures cut fractures filled with fluorite and barite. **d)** RCC-09-14-80.1 m, pyrite aggregates with bastnäsite-(Ce), crandallite and synchysite-(Ce). **e)** Euhedral pyrite aggregates with altered apatite, synchysite-(Ce) and barite in dolomite. **f)** RCC-09-14-121.2 m, late calcite veins cut barite and synchysite-(Ce) vein. Dol: dolomite, Fl: fluorite, Py: pyrite, Hem: hematite, Brt: barite, Bas: bastnäsite, Syn: synchysite, Crd: crandallite group mineral, Ap: apatite.

Table 1. List of minerals detected by Powder-XRD in samples from vertical drill hole RCC-09-14. Relative qualitative abundance of minerals is expressed in terms of height of their diagnostic peek.

Depth (m)	Dol	Cal	Fl	Brt	Py	Mc	Qtz	Ap	Bas	Mnz
1-6	+++	+	++	++	+		+		++	+
6-9	+++	++	++	+	++	+	+			
9-12	+++	++	++	+	++	+				
12-15	+++	++	++	+	++		+			
15-18	+++		++	+	+				++	
18-21	+++		++	++	+		+		++	
21-24	+++		++	++	+				++	+
24-27	+++		++	+	+				+	
27-30	+++		++	+	+				+	
30-33	+++		++	++	+				++	
33-36	+++		++	+	++		+		++	
36-39	+++		++	+	+	+	+		+	
39-42	+++		++	+	++	+	+			
42-45	+++		++	+	+	+	+		++	
45-48	+++		++	+	+		+			
57-60	+++		++	+	+		+		+	
60-63	+++		++	+	+	+	+		+	
63-66	+++		++	+	++		+			
66-69	+++		++	+	+		+		+	
69-72	+++		++	+	++		+		+	
72-75	+++		++	+	+		+			
75-78	+++		++	++	+		+			
78-81	+++		++	+	++		+			
81-84	+++		++	+	++					
84-87	+++		++	+	++		+		+	
87-90	+++		++	+	++		+			
90-93	+++		+	+	++					
93-96	+++		+	+	++					
96-99	+++		+	+	++		+			
99-102	+++		+	+	+		+			
102-105	+++		++	+	++		+			
105-108	+++		++	+	++		+			
108-111	+++		++	+	++		+			
111-114	+++			+	++		+			
114-117	+++		++	+			+	+	+	
117-120	+++		++	+			+		++	
120-123	+++		++	+			+		++	
123-124.7	+++		+	+			+	+	++	

Dol: dolomite, Cal: calcite, Fl: fluorite, Brt: barite, Py: pyrite, Mc: microcline,
Qtz: quartz, Ap: fluorapatite, Bas: bastnasite, Mnz: monazite
+++ : peak high, ++ : peak middle, + : peak low

Table 2. Sample descriptions and REE minerals detected by SEM-EDS in drill hole RCC-09-14. Mineral abundances: +++ major, ++ minor, + trace.

Sample Number	Rock Type	Microscopic observations	REE minerals	Other minerals	REE content
RCC-09-14_1	Dolostone (Fe oxide-stained), weathered	fg dolomitic limestone; REE carbonates and phosphates with pyrite, fluorite and barite; late calcite vein	REE carbonates++, REE phosphates+++	dolomite+++, barite+++, fluorite++, calcite++, pyrite+	high
RCC-09-14_2.8	Fluorite-bearing Fe oxide stained dolostone breccia	altered cg dolomitic limestone. REE carbonates and REE phosphates occur with pyrite, fluorite and barite; late calcite veinlets	REE carbonates++, REE phosphates+++,	dolomite+++, barite++, fluorite+++, calcite++, pyrite+	high
RCC-09-14_5.8	Fluorite-bearing, Fe oxide stained dolostone	fg dolostone, REE carbonates and phosphates occur with pyrite, fluorite and barite; late stage fg pyrite aggregates; calcite vein is the latest	REE carbonates++, REE phosphates++	dolomite+++, barite++, fluorite+++, calcite++, pyrite+++	moderate
RCC-09-14_6.75	Fluorite-bearing, pale gray dolostone cut by calcite vein.	contact of altered fg dolostone with calcite vein; REE carbonates occur with pyrite, fluorite and barite; late veinlets consisting of fg pyrite aggregates	REE carbonates+	dolomite+++, barite++, fluorite+++, calcite+++, pyrite++	low
RCC-09-14_8.15	Fluorite-, pyrite-bearing pale gray dolostone cut by calcite vein	contact of altered fg dolostone with calcite vein. REE carbonates occur with pyrite, fluorite and barite; late veinlets containing fg pyrite aggregates	REE carbonates+	dolomite+++, barite+, fluorite+++, calcite+++, pyrite+++, K-feldspar+	low
RCC-09-14_8.5	Fluorite and pyrite-bearing whitish limestone, calcite vein	altered cg dolostone. REE carbonates and REE phosphates occur with pyrite, fluorite and barite; late veinlets containing fg pyrite aggregates	REE carbonates+, REE phosphates+	dolomite+++, barite+, fluorite+++, calcite+, pyrite+++	low
RCC-09-14_37.3	Fluorite-bearing dolostone; cut by cg calcite vein	altered fg dolostone; REE carbonates and phosphates with fluorite, barite, and pyrite	REE carbonates+, REE phosphates+	dolomite+++, barite+++, fluorite+++, quartz++, K-feldspar++, calcite+, pyrite++	low
RCC-09-14_40.4	Fluorite- and pyrite-bearing grey limestone	altered fg dolomitic limestone; apatite grains are cut by fluorite-filled fractures		dolomite+++, barite++, apatite+++, fluorite+++, quartz++, K-feldspar++, pyrite+++	low
RCC-09-14_69.6	Fluorite- and pyrite-bearing grey dolostone, calcite veinlets, with massive pyrite	altered fg dolostone; REE carbonates occur with fluorite, barite and pyrite. Late veinlets containing fg pyrite aggregates	REE carbonates++	dolomite+++, barite++, fluorite+++, quartz++, K-feldspar++, pyrite+++	moderate

Table 2. Continued.

RCC-09-14_80.1	Fluorite- and pyrite-bearing grey dolostone	altered fg dolostone; REE carbonates and phosphates occur with fluorite, barite, and pyrite; apatite is common; late fg pyrite aggregates	REE carbonates++, REE phosphates+	dolomite+++, barite++, apatite +++, fluorite++, K-feldspar++, pyrite+++	moderate
RCC-09-14_108.6	Fluorite and pyrite-rich grey dolostone	fg dolostone; REE carbonates accompanied by fluorite, pyrite and barite; fg pyrite aggregates	REE carbonates+++, REE phosphates+	dolomite+++, barite++, fluorite++, pyrite+++	high
RCC-09-14_120	Whitish dolostone	cg dolostone; REE carbonates and phosphates occur with fluorite, pyrite, and barite; apatite is common	REE carbonates++, REE phosphates+	dolomite+++, barite++, fluorite++, pyrite++	moderate
RCC-09-14_121.2	Whitish dolostone	fg dolostone; REE carbonates and phosphates occur with fluorite, pyrite, and barite; apatite is common; fg pyrite aggregates; late calcite veinlets	REE carbonates+++, REE phosphates+	dolomite+++, barite++, apatite +++, fluorite++, pyrite++	high
RCC-09-14_121.6	Fluorite-bearing whitish dolostone	cg dolostone; REE carbonates and REE phosphates with fluorite coexist pyrite and barite; fg pyrite aggregates; late calcite vein	REE carbonates+++, REE phosphates+++	dolomite+++, barite++, fluorite++, pyrite++	high
RCC-09-14_124.7	Whitish dolostone	cg recrystalized dolostone; REE carbonates with fluorite, pyrite and barite; apatite is common	REE carbonates+++	dolomite+++, barite++, apatite +++, fluorite++, pyrite++	high

cg-coarse grain, fg-fine grain

Table 3. Representative composition of bastnäsite from drill hole RCC-09-14. Concentrations of Si, Al, Na, Mg, Fe, Ba, and Y were not detected by SEM-EDS analysis. Results in wt.%, normalized to 100 wt.%.

(wt %)	RCC-09-14-1m	RCC-09-14-1m	RCC-09-14-1m	RCC-09-14-1m	RCC-09-14-1m	RCC-09-14-1m	RCC-09-14-80.1m	RCC-09-14-80.1m	RCC-09-14-108.1m	RCC-09-14-108.1m	RCC-09-14-108.1m	RCC-09-14-121.2m
Ca	-	-	0.72	0.67	0.90	-	1.76	2.01	2.13	2.81	1.90	1.19
Sr	1.63	2.07	-	2.03	-	-	-	-	-	1.01	-	-
Mn	-	-	-	-	-	-	-	-	-	-	0.79	-
As	-	-	-	0.93	-	-	-	-	-	-	-	-
La	19.81	22.1	20.8	18.47	22.09	26.7	8.72	9.37	20.28	19.05	19.47	24.93
Ce	33.83	34.41	30.77	29.97	33.45	33.56	24.31	24.69	28.53	27.92	28.84	32.44
Pr	3.38	-	2.53	2.33			4.72	4.27	-	-	-	2.81
Nd	10.6	10.86	11.68	10.61	10.27	8.18	24.06	22.61	8.38	8.69	10.62	8.32
Sm	-	-	-	-	-	-	2.84	2.56	-	-	-	-
Th	-	-	2.24	3.11	2.61		2.30	3.09	8.42	6.88	6.66	-
O	22.43	21.79	22.55	22.45	21.93	22.35	22.85	23.71	21.63	24.55	23.03	21.58
S	-	-	-	-	-	-	-	-	0.86	-	-	-
F	8.33	8.77	8.72	9.43	8.75	9.2	8.43	7.69	9.77	9.09	8.68	8.73
Total	100.0	100	100	100	100	100	100	100	100	100	100	100

Table 4. Representative composition of synchysite from drill hole RCC-09-14. Concentrations of P, Na, Mg, Sr, Mn, As, Fe, Ba, Sm and S were not detected by SEM-EDS analysis. Results in wt.%, normalized to 100 wt.%.

(wt %)	RCC-09-14-1m	RCC-09-14-1m	RCC-09-14-1m	RCC-09-14-1m	RCC-09-14-5.8m	RCC-09-14-5.8m	RCC-09-14-5.8m	RCC-09-14-5.8m	RCC-09-14-5.8m	RCC-09-14-5.8m	RCC-09-14-5.8m	RCC-09-14-5.8m	RCC-09-14-80.1m	RCC-09-14-80.1m	RCC-09-14-80.1m	RCC-09-14-80.1m	RCC-09-14-121.2m	RCC-09-14-121.2m	RCC-09-14-121.2m
Si	-	-	-	-	-	-	-	-	-	-	-	-	-	0.87	-	-	-	-	-
Al	-	-	-	-	-	-	-	-	-	-	-	-	-	-	-	0.51	-	-	-
Ca	14.42	14.45	12.83	14.97	14.56	15.46	15.5	16.12	14	15.7	13.66	13.66	15.53	14.59	14.25	14.37	14.07	14.61	11.19
Y	-	-	-	-	2.13	1.44	-	-	-	-	-	-	-	-	-	-	-	-	-
La	12.82	12.32	17.41	13.03	11.16	13.00	14.75	12.3	15.61	15.36	15.53	16.07	5.23	5.82	14.4	13.85	15.94	15.55	20.23
Ce	23.35	23.43	25.27	23.41	23.82	24.05	24.73	24.22	23.29	23.52	24.07	25.25	17.68	16.65	21.07	19.18	24.79	24.19	24.09
Pr	-	-	-	-	2.92	-	-	-	-	-	8.3	7.27	-	-	-	-	-	2.77	-
Nd	6.95	9.11	6.17	8.41	10.21	8.38	6.20	8.45	7.01	6.79	2.58	2.75	18.5	19.4	9.18	9.49	8.00	6.44	8.34
Th	1.89	1.74	2.76	3.30	-	-	1.28	1.70	3.70	2.82			2.82	3.30	3.15	3.34	-	-	-
O	33.72	32.59	27.99	30.52	28.64	31.35	31.8	31.41	30.34	30.28	30.58	28.56	33.49	33.67	31.35	33.27	31.31	30.06	29.18
F	6.86	6.36	7.58	6.35	6.56	6.32	5.74	5.81	6.04	5.54	5.27	6.44	6.74	5.69	6.6	5.99	5.89	6.38	6.96
Total	100	100	100	100	100	100	100	100	100	100	100	100	100	100	100	100	100	100	100

Table 5. Representative composition of parisite from drill hole RCC-09-14. Concentrations of P, Si, Al, Na, Mg, Mn, As, Fe, Ba, Y, Sm and S were not detected by SEM-EDS analysis. Results in wt.%, normalized to 100 wt.%.

	RCC09-14-121.1m	RCC09-14-121.1m
Ca (wt %)	8.41	8.48
Sr	0.85	-
La	14.99	19.14
Ce	24.69	30.80
Pr	3.04	-
Nd	7.90	8.04
Th	5.40	-
O	22.44	26.04
F	12.27	7.50
Total	100	100

Table 6. Representative composition of monazite from drill hole RCC-09-14. Concentrations of Si, Na, Mg, Mn, As, Fe, Y, Pr, and Sm were consistently below the lower limit of detection. Results in wt.%, normalized to 100 wt.%.

	RCC09-14-1m	RCC09-14-1m	RCC09-14-5.8m	RCC09-14-5.8m	RCC09-14-5.8m	RCC09-14-5.8m	RCC09-14-5.8m
P (wt %)	11.17	13.03	11.03	12.69	12.33	12.31	12.75
Al	-	6.35	4.79	-	5.33	6.75	4.22
Ca	4.20	1.60	3.34	2.28	1.33	1.82	1.17
Sr	-	2.82	2.54	-	3.09	2.43	2.83
Ba	-	-	-	1.89	-	-	-
La	18.95	14.15	15.76	18.66	15.69	15.00	16.36
Ce	32.98	21.69	21.46	26.75	22.64	22.48	23.79
Nd	8.38	5.32	6.20	8.80	5.72	4.01	5.49
Th	3.55	-	-	1.99	1.54	-	1.75
O	20.78	34.28	33.4	26.94	31.55	34.28	31.21
S	-	0.76	0.52	-	0.78	0.92	0.43
F	-	-	0.95	-	-	-	-
Total	100	100	100	100	100	100	100

Table 7. Representative composition of crandallite group minerals from drill hole RCC-09-14. Concentrations of Na, Mg, Mn, As, Fe, Ba, Y, Pr, Sm and Th were consistently below the lower limit of detection. Results in wt.%, normalized to 100 wt.%.

	RCC09-14-5.8m	RCC09-14-80.1m	RCC09-14-80.1m	RCC09-14-121.2m	RCC09-14-121.2m
P (wt %)	9.92	10.88	11.55	11.33	11.25
Si	-	1.72	-	-	-
Al	16.76	20.94	17.88	17.58	17.77
Ca	6.13	3.69	3.35	3.32	2.30
Sr	5.49	-	6.22	7.84	10.74
La	9.83	-	-	4.19	3.50
Ce	8.31	3.06	6.37	5.77	3.70
Nd	-	3.31	-	-	-
O	35.78	52.88	52.79	48.69	48.68
S	1.59	2.34	1.85	1.28	2.07
F	6.18	1.18	-	-	-
Total	100	100	100	100	100

veinlets. Late calcite veinlets cut fractures filled with fluorite and barite and also cut monominerallic pyrite veinlets that postdate fluorite-barite filled fractures (Fig. 3c). Apatite, with dissolution-induced porosity (Fig. 3e) was observed in 4 thin sections (RCC-09-14 40.4, 80.1, 121.2, 124.7).

Bastnäsite-(Ce) contains 8.7 to 26.7 wt.% La, 24.3 to 34.4 wt.% Ce and undetected to 4.7 wt.% Pr, 8.2 to 24.1 wt.% Nd, undetected to 2.8 wt.% Sm, and undetected to 8.4 wt.% Th (Table 3). Synchysite-(Ce) includes 5.2 to 17.4 wt.% La, 16.7 to 25.3 wt.% Ce, undetected to 8.3 wt.% Pr, 2.6 to 19.4 wt.% Nd, undetected to 2.1 wt.% Y and undetected to 3.7 wt.% Th (Table 4). Representative chemical compositions of parisite are shown in Table 5.

Monazite-(Ce) contains 11.03 to 13.03 wt.% P, 14.15 to 18.95 wt.% La, 21.46 to 32-98 wt.% Ce, 4.01-8.80 wt.% Nd, and undetected to 3.55 wt.% Th (Table 6).

The crandallite group mineral contains 9.9 to 11.6 wt.% P, 16.8 to 20.9 wt.% Al, 2.3 to 6.1 wt.% Ca, undetected to 10.7 wt.% Sr, undetected to 9.8 wt.% La, 3.1 to 8.3 wt.% Ce, and undetected to 3.3 wt.% Nd (Table 7). The Raman spectroscopy analysis of the crandallite group mineral shows a mixture of peaks attributable to crandallite, goyazite, and florencite. The crandallite group mineral displays a porous texture and variable chemical composition.

4. Discussion

This mineralogical study supplements the summary of previously published data presented by Green et al. (2017) and confirms that fluorocarbonates and Al-containing phosphates of crandalite group are the main REE-carriers. Both REE carbonates and REE-bearing Al-phosphates are commonly spatially associated with pyrite, barite, and fluorite (Figs. 3a-f). Detailed paragenetic studies are ongoing.

4.1. REE-bearing fluorocarbonates

Bastnäsite-(Ce), synchysite-(Ce) and parisite-(Ce) were identified at the Rock Canyon Creek deposit. Bastnäsite-(Ce) and synchysite-(Ce) are expected to have variable REE content (Fleisher, 1978; Hoshino et al., 2016). Concentrations exceeding 20 wt.% Nd in bastnäsite-(Ce) (sample RCC-09-14 80.1 m); Table 3) are uncommon in carbonatites, granites, and pegmatites but would be expected in hydrothermal deposits (Fleischer, 1978). Concentration of Nd in synchysite (sample RCC-09-14 80.1 m; Table 4) reaches more than 19 wt.%.

As generally reported in the literature, bastnäsite contains <0.3% Th, synchysite <0.8% Th and parisite <1.3% Th (Hoshino et al., 2016). Although REE fluorocarbonates from Rock Canyon Creek contain up to 8.4 wt.% Th, petrographic work failed to reveal visible Th-rich mineral inclusions in these minerals. If such inclusions exist, they must be submicroscopic. Alternatively, Th may be incorporated into the crystal structure of these REE-bearing fluorocarbonates.

4.2. REE-bearing phosphates

Crandallite group minerals, apatite and monazite were identified in this study, and the importance of crandallite group minerals as REE-carriers was confirmed.

Unreported in previous studies (Green et al., 2017), the Monazite-(Ce) documented in this study is texturally and chemically heterogeneous, and incorporating substantial concentrations of Al, Ca and Sr (Table 6). Monazite-(Ce) is commonly mixed with REE fluorocarbonates, crandallite and/or barite (hydrothermal mineralization). It is anhedral, porous in appearance, and fractured. Zoning and embayed boundaries are shown on Figure 3b. Although identifying monazite solely by its chemical composition is difficult, its presence was confirmed by Raman spectroscopy. The composition of monazite is highly

variable and it is probably of secondary origin.

In the Rock Canyon Creek deposit, porous apatite occurs with pyrite, barite, fluorite and REE fluorocarbonates (Fig. 3e), and as disseminated porous grains in dolomite suggesting that it is a primary mineral. Regardless of its origin, apatite commonly contains less than 1 wt.% of ΣREE. The chemical composition of apatite from Rock Canyon Creek will be reported in future studies.

The crandallite group minerals belong to the crandallite-goyazite-florencite solid solution (Table 7). At Rock Canyon Creek, these minerals occur in veinlets. The porous texture and variable chemical composition suggest that the crandallite group minerals probably formed by relatively low-temperature hydrothermal, possibly retrograde, processes. Observed mineral associations suggest that most of the REE-bearing fluorocarbonates in drill hole RCC-09-14 are of hydrothermal origin, along with fluorite, barite, and pyrite. The crandalite group minerals, and possibly monazite, may be of retrograde or supergene origin. The variations in composition of individual REE-bearing minerals probably reflect changes in, for example, the temperature, alkalinity, and composition of hydrothermal fluids or position of the samples in the mineralizing system. Involvement of both hypogene and supergene fluids is possible.

5. Future laboratory work

Further mineralogical analyses of samples from drill holes RCC-09-14, RCC-09-10, and RCC-09-02 that intersected the Rock Canyon Creek mineralization will be performed at the Institute for Geo-resources and Environment, Geological Survey of Japan, National Institute of Advanced Industrial Science and Technology in Japan. The following methods will be used.

- Chemical analysis of REE-bearing minerals and major minerals by laser ablation inductively coupled plasma mass spectrometry (LA-ICP-MS).
- Determination of modal abundance of REE minerals in the representative thin sections by automated scanning electron microscope based mineral liberation analysis (MLA).
- Mg isotope analysis of fluorite, calcite and limestone by multi collector ICP-MS.

Acknowledgments

This paper is a result of cooperation between the Geological Survey of Japan, British Columbia Geological Survey (also part of the Specialty Metal Component of the Targeted Geoscience Initiative 5; spearheaded by Natural Resources Canada), and Mr. Chris Graf and Spectrum Mining Corporation, the owners of the Rock Canyon Creek deposit. We thank Mr. Chris Graf for guidance in the field, permission to sample the core, and enriching discussions. Ms. Fiona Katay (British Columbia Ministry of Energy and Mines, Cranbrook) provided invaluable field survey and core logging support.

References cited

Green, C., Simandl, G.J., Paradis, S., Katay, F., Hoshino, M., Kon, Y., Kodama, S., and Graf, C., 2017. Geological setting of the Rock Canyon Creek REE-fluorite deposit, British Columbia, Canada. In: Geological Fieldwork 2016, British Columbia Ministry of Energy and Mines, British Columbia Geological Survey Paper 2017-1, this volume.

Fleisher, M., 1978. Relative proportions of lanthanides in minerals of the bastnaesite group, Canadian Mineralogist, 16, 361-363.

Hora, Z.D., and Kwong, Y.D.J., 1986. Anomalous rare earth elements (REE) in the Deep Purple and Candy claims. In: Geological Fieldwork 1985, British Columbia Ministry of Energy, Mines, and Petroleum Resources, British Columbia Geological Survey, , Paper 1986-1, pp. 241-242.

Hoshino, M., Sanematsu, K., and Watanabe, Y., 2016. REE mineralogy and resources. Handbook on the Physics and Chemistry of Rare Earths, Elsevier: Amsterdam, 49, Chapter 249, pp. 129-291.

Pell, J., 1994. Carbonatites, nepheline syenites, kimberlites and related rocks in British Columbia. British Columbia Ministry of Energy, Mines, and Petroleum Resources, British Columbia Geological Survey, Bulletin 88, 44p.

Pell, J., and Hora, Z.D., 1986. Geology of the Rock Canyon Creek fluorite/rare earth element showing southern Rocky Mountains (82J/3E). In: Geological Fieldwork, 1986,British Columbia Ministry of Energy, Mines and Petroleum Resources, British Columbia Geological Survey Paper 1987-1, pp. 255-258.

Pighin, D.L., 2010. Assessment Report Rock Canyon Property, British Columbia Geological Survey Assessment Report 31435. 109p.

Simandl, G.J., Prussin, E.A., and Brown, N., 2012. Specialty metals in Canada. British Columbia Ministry of Energy, Mines and Natural Gas, British Columbia Geological Survey Open File 2012-7, 48p.